Applied Catalysis B: Environmental 194 (2016) 150–156

Contents lists available at ScienceDirect

Applied Catalysis B: Environmental

journal homepage: www.elsevier.com/locate/apcatb

# Rapid photocatalytic debromination on $TiO_2$ with *in-situ* formed copper co-catalyst: Enhanced adsorption and visible light activity

Yanhui Lv, Xiaofeng Cao, Haiying Jiang, Wenjing Song, Chuncheng Chen*, Jincai Zhao*

*Beijing National Laboratory for Molecular Sciences, Key Laboratory of Photochemistry Institution Institute of Chemistry, Chinese Academy of Sciences, Beijing 100190, China*

ARTICLE INFO

*Article history:*
Received 7 March 2016
Received in revised form 25 April 2016
Accepted 26 April 2016
Available online 28 April 2016

*Keywords:*
Copper nanoparticles
$TiO_2$
Photocatalytic debromination
Visible light
Cocatalyst

ABSTRACT

The cheap metal Cu particles *in-situ* loaded on $TiO_2$ surface is able to co-catalyze the photocatalytic debromination of polybrominated pollutants. Over 15 times of enhancement for the reductive debromination of deca-brominated diphenyl ether (BDE209) over $Cu/TiO_2$ is achieved, relative to that on the bare $TiO_2$. Moreover, the presence of metal copper markedly changes the distribution of the formed intermediates, indicating the change in the debromination mechanism because of the co-catalysis of metal Cu. The detailed *ex-situ* and *in-situ* characterizations of the $Cu/TiO_2$ photocatalyst indicate that the copper remains its $Cu^0$ valence state in photocatalytic turnover. The mechanistic investigation suggests that the presence of metal copper nanoparticles greatly enhance the adsorption of hydrophobic BDE209 on the photocatalyst, which facilitates the electron transfer from the conduction band of $TiO_2$ to the pollutants. Our experimental results also implies that the interaction of BDE209 with metal copper co-catalyst would position-specifically activate the C-Br bonds during the dissociative electron transfer. We further show that the surface plasmon resonance of metal copper can contribute to the enhancement of photocatalytic activity by utilizing the visible-light part of the irradiation. The present study provides a simple and economic method for elimination of organobromide pollutants, and would be promising in reductive dehalogenation by other techniques.



## 1. Introduction

As a class of brominated flame retardants, polybrominated diphenyl ethers (PBDEs) have been extensively used in electronics, plastic products, furniture, automotives, textiles and foam over the past several decades [1–4]. These PBDEs are readily released from products to the environment, since they are simply blended with the polymer during the manufacturing process. As a result, PBDEs are commonly detected in water, sediment/soil, air, biota, animals (rats, fish, marine mammals *etc.*), even in human blood, milk and tissues [5–9]. Even worse, recent studies show that many PBDEs are quite toxic to animals. For example, they can cause endocrine disruption, neurotoxic and immunotoxic effects in numerous species [10–12]. The ubiquity and toxicity of PBDEs triggered the substantial investigations on the development of efficient techniques to degrade these types of pollutants.

Due to their strong intractability to oxidative degradation, most studies for the degradation of PBDEs are based on the reductive debromination by such as biotic reductive debromination [13–15], zero−valent iron (ZVI) [16–18], sodium borohydride [19], electrochemistry [20], and hydrothermal treatment [21]. In our previous studies, we found that the conduction band electrons generated in UV-irradiated $TiO_2$ photocatalyst can be used to reduce deca-brominated diphenyl ether (BDE209) to its lower brominated congeners [22,23]. However, the debromination of the less brominated congeners became rather difficult on the bare $TiO_2$. To realize the complete debromination of BDE209 to diphenyl ether, noble metal Pd as a co-catalyst is required [24]. It is still desirable to explore cheaper metal to replace noble metals as co-catalysts.

One of major challenges for photocatalytic degradation of hydrophobic substrate such as BDE209 is their weak interaction with the strongly hydrophilic surface of metal oxide semiconductors, which is quite unfavorable for the interfacial hole/electron transfer between the substrate and photocatalyst. Therefore, surface modification that strengthens the interaction between the photocatalyst and the substrate would significantly facilitate the photocatalytic reduction of these hydrophobic aryl halides. The copper species ($Cu^+$ or $Cu^0$) has been used as a catalyst for Ullmann coupling reaction of halogenated compounds, in which $Cu^+$ or $Cu^0$ can insert the C—X bond and catalyze the dehalogenated

* Corresponding authors.
*E-mail addresses:* ccchen@iccas.ac.cn (C. Chen), jczhao@iccas.ac.cn (J. Zhao).

http://dx.doi.org/10.1016/j.apcatb.2016.04.053
0926-3373/

coupling reaction. They were also loaded on $TiO_2$ photocatalyst to improve the photocatalytic efficiency of hydrogen production [25,26], photodegradation of organic pollutants [27,28], and carbon dioxide reduction [29,30]. Particularly, the CuO/$TiO_2$ nanocomposites were recently reported to enhance the photocatalytic reductive degradation of PBDEs. Such an enhancement is attributed to the more negative potential of the *in-situ* formed $Cu_2O$, which makes the reduction of PBDEs thermodynamically favorable [31]. However, no study on the coupling of the metal copper catalysis with the photocatalytic reduction dehalogenation has been done, and the co-catalysis effect of metal Cu that activates kinetically the C—Br bond cleavage is not accessible so far. In this work, we report that the *in-situ* loaded metal Cu particles on $TiO_2$ surface can greatly enhance the absorption of the BDE209. In concert with the co-catalytic dehalogenation properties and the visible-light utilization by surface plasmon resonance of metal copper, over 15-times efficiency enhancement is achieved for the photocataytic debromination of BDE209. The intermediate analysis, the *in-situ* and *ex-situ* characterization of the state of copper species were also performed in details to demonstrate the site-dependent photocatalytic debromination mechanism. This study proposes a facile, efficient method for rapid/selective debromination of polybrominated organic compounds, towards the utilization of full solar irradiation, which may be extended to other photocatalytic reactions of halogenated pollutants.

## 2. Experimental section

### 2.1. Materials

$TiO_2$ (anatase, 99.9%; surface area 116 $m^2 \cdot g^{-1}$) was supplied by the Alfa Aesar (United States). Anhydrous cupric chloride (99.995%, ultra dry) and cuprous chloride (99.999%) also were purchased from Alfa Aesar (United States). Decabromodiphenyl ether (BDE209), Decabromobiphenyl (DBB), Hexabromo benzene (HBB) and Pentabromophenol (PBP) were purchased from Aldrich Chemical Co. (Milwaukee, WI). A standard solution of PBDEs (EO5103) was purchased from Cambridge Isotope Laboratories (CIL, And over, MA). Tetrahydrofuran was analytical reagent and methanol was a guaranteed reagent (Chemical Co., Beijing). They were used without further purification. Deionized and doubly distilled water was used throughout the study.

### 2.2. Photocatalytic reactions

BDE209 stock solution ($1 \times 10^{-3}$ mol $L^{-1}$) in tetrahydrofuran was diluted to $1 \times 10^{-5}$ mol $L^{-1}$ with methanol solvent. To distinguish and highlight the enhancement of the copper species on the photoreaction, much less $TiO_2$ (0.2 g/L *vs.* 1 g/L in our previous study [22]) was used. The photocatalytic reaction was carried out in freshly prepared 25 mL BDE209 methanol solution with or without $CuCl_2$ (the mass ratios of $Cu^{2+}$:$TiO_2$ from 0 to 0.48%) in Pyrex vessel with a volume of 60 mL. The vessel was sealed with a rubber septum under Ar. Before the light irradiation, the suspensions were firstly ultrasonically dispersed in dark for 10 min, then magnetically stirred for 20 min to reach the adsorption–desorption equilibrium, finally purged with argon for 30 min to remove $O_2$ and protected under an argon atmosphere. Reaction suspensions were magnetically stirred during the irradiation at 25 ± 0.2 °C (controlled by cooling circulation water). Light source was a 300 W Xenon lamp (CEL–HXF300, Beijing) with an infrared cutoff filter (to minimize the thermal effect), a 360 nm cutoff filter (to prevent the direct photolysis of BDE209), and the light intensity was about 30 mW $cm^{-2}$. At given time intervals, 1 mL suspensions were sampled and centrifuged immediately to remove the photocatalyst particles, and the supernatants at were analyzed by the HPLC (Agilent 1260) analysis with a UV detector at 240 nm, using Dikma Platisil ODS C–18 column (250 mm × 4.6 mm, 5 μm film thickness). The mobile phase was 100% methanol with a flow rate of 1.0 mL $min^{-1}$. The quantification was done with a calibration cure with BDE209 standard. The photocatalytic degradation of DBB, HBB, PBP was carried out under the same experimental conditions as that of BDE209. To test the reproducibility and uncertainty of the degradation experiments, the photochemical reactions were repeated three times.

### 2.3. Intermediate analysis

The intermediate distribution during the photocatalytic degradation of BDE209 was investigated by gas chromatography (Agilent 7890A) coupled with a micro–electron capture detector (GC–μECD). The carrier gas was helium at a constant flow rate of 1.0 mL $min^{-1}$. The injection temperature was 300 °C, and the detector temperature was 320 °C. The oven temperature was controlled by the following program: kept at 100 °C for 2 min, increased at a rate of 15 °C $min^{-1}$ to 230 °C, 5 °C·$min^{-1}$ to 270 °C, 10 °C·$min^{-1}$ to 320 °C and kept at this temperature for 12 min. The bromide ion ($Br^-$) concentration was investigated by a DX-900 Ion Chromatograph (IC) with an IonPac AS23 column (Dionex). The eluent for the IC was a 20 mM KOH solution, the curb was 20 mA, and the flow rate was 1.0 mL/min. The identification by IC analysis was performed using an observed retention time of approximately 9.3 min.

### 2.4. Characterization methods

Ultraviolet–visible diffuse reflectance spectroscopy (UV–vis DRS) of *ex-situ* Cu/$TiO_2$ powders (prepared by photodeposition, centrifugation and drying) and *in-situ* Cu/$TiO_2$ suspensions (Cu metal particles were *in-situ* photodeposited on $TiO_2$, which were still in the suspensions) were performed on Hitachi U–3010, $BaSO_4$ and original $Cu^{2+}$/$TiO_2$ suspension were used as reference, respectively. X–ray diffraction (XRD) measurements were performed on a Regaku D/Max–2500 diffractometer with a Cu *Ka* radiation source (1.5406 Å). Diffraction patterns were recorded from $2\theta$ = 10 to 80 with a step size of 0.04 at 4 $min^{-1}$. X-ray photoelectron spectroscopy (XPS) were recorded with an ESCALab220i–XL electron spectrometer from VG Scientific using a 300 W Al *Kα* radiation. The base pressure was about $3 \times 10^{-9}$ mbar. The binding energies were referenced to the C1s line at 284.8 eV from adventitious carbon. A high–resolution transmission electron microscope (HR–TEM, JEM 2010F) were operated at an accelerating voltage of 200 kV.

## 3. Results and discussion

### 3.1. Enhanced photocatalytic debromination of BDE209 on Cu/$TiO_2$

The photoreductive debromination of BDE209 on bare $TiO_2$ and Cu/$TiO_2$ systems was investigated in methanol, which was used as both the solvent and electron donor. To avoid the direct photolysis of BDE209, an irradiation with λ > 360 nm was employed. Relative to the slow degradation of BDE209 on bare $TiO_2$, the presence of $Cu^{2+}$ in the $TiO_2$ suspension significantly accelerated the debromination reaction, and the acceleration extent was dependent on the $Cu^{2+}$ contents (Fig. 1A). The optimal photocatalytic activities reached at the $Cu^{2+}$ content of 0.16 wt%. It is also noted that an induction period (at the beginning of *ca.* 5 min) appeared during the degradation of BDE209 in the presence of $Cu^{2+}$, in which $Cu^{2+}$ was photocatalytically reduced to $Cu^0$ on the $TiO_2$ surface. Degradation rate constant *k* is fitted by pseudo–first–order kinetics (the data point before 5 min was not included due to the presence of induction period). As shown in Fig. 1B, the fitted rate constant *k* on

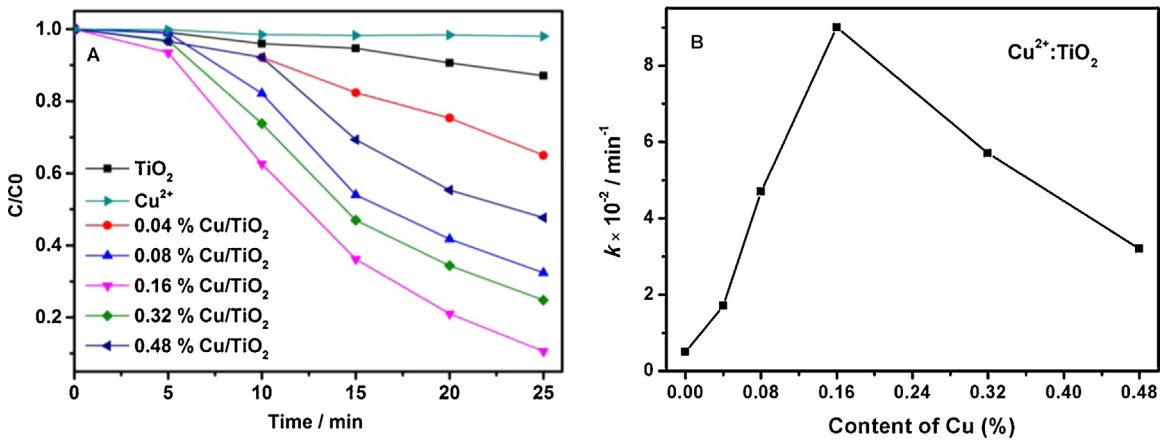


**Fig. 1.** (A) Temporal curves of the photoreductive debromination of BDE209 on $TiO_2$, $Cu^{2+}$ and $Cu/TiO_2$ system with various Cu contents (Cu:$TiO_2$ from 0.04 ~ 0.48 wt%), under Xe lamp irradiation and argon protection; (B) change of the apparent first-order rate constants $k$ against the loading content of Cu.

0.16% $Cu/TiO_2$ is 0.090 $min^{-1}$, which is 16 times as that on pristine $TiO_2$ ($k$ = 0.005 $min^{-1}$). In addition, an examination on the concentrations of $Br^-$ indicates that, as shown in Fig. S1, the release of the $Br^-$ is much rapider (by about 12 times) in the $Cu/TiO_2$ system than that over bare $TiO_2$, which is in well agreement with the enhanced reduction of the BDE209.

As a control, the presence of $Cu^{2+}$ without $TiO_2$ did not show any activity for debromination under irradiation, indicating that the increased photocatalytic activity is attributed to the co-catalysis of copper species. In another experiment, metal Cu particles was pre-deposited on $TiO_2$ surface by irradiating the deaerated $Cu^{2+}/TiO_2$ methanol suspension, and the pre-loaded $Cu/TiO_2$ was separated out by centrifugation. Using these $Cu/TiO_2$ powders as photocatalysts, the photocatalytic reduction of BDE209 exhibited a similar enhancement to that over *in-situ* formed $Cu/TiO_2$, except that the induction period was not observable any more (Fig. S2). The stability of photocatalyst during the catalytic reaction was examined by adding BDE209 repeatedly into the $Cu/TiO_2$ suspension once the BDE209 was degraded completely. As shown in Fig. 2A, after four cycles, the $Cu/TiO_2$ photocatalyst exhibited only a slight loss of debromination activity, confirming that $Cu/TiO_2$ is considerably stable. Furthermore, the turnover number (TON) of copper after four cycles was calculated to be 16, assuming that all the added copper atoms were involved in the photocatalytic reaction and only one bromine atom was removed from BDE209. These results confirmed that copper acted as cocatalyst, rather than a stoichiometric reagent.

The cocatalysis of copper with $TiO_2$ is not only applicable to polybrominated diphenyl ethers, but also to the enhanced photocatalytic reduction of other polybrominated aryl pollutants such as decabromobiphenyl (DBB), hexabromobenzene (HBB) and pentabromophenol (PBP). The photoreductive debromination activity of DBB, HBB, and PBP are promoted by about 9, 8 and 6 times over $Cu/TiO_2$ (16%) relative to that on bare $TiO_2$, respectively (Fig. 2B–D).

### 3.2. Characterization of $Cu/TiO_2$

During photocatalytic reduction reactions, the color of the suspensions was observed to become pink, corresponding to the light absorption by the surface plasmon resonance (SPR) of metal copper particles. To verify that, the photocatalyst was separated after the photocatalytic reaction and UV–vis DRS was employed to examine the absorption of photocatalyst. Consistent with the color change, an absorption peak at 578 nm was detected (Fig. 3A), which is a SPR characteristic of $Cu^0$ particle [26]. With the increased concentration of the initial $Cu^{2+}$, the peak at 578 nm was gradually enhanced, and the pink color of the suspensions after UV irradiation became deeper gradually, as shown in Fig. 3A Inset. From the XRD of $Cu/TiO_2$ particles Fig. 3B, it can be found that the diffraction peaks of the (111), (200) and (220) planes of metal Cu (PDF No. 85-1326) were observed for the $Cu/TiO_2$ samples with 1.6% and 16% of Cu content, although the peaks for metal Cu were hardly detected for the sample with 0.16% of Cu because of its low content. The Cu2p XPS of $Cu/TiO_2$ sample showed that only two signal peaks at 932.0 eV and 932.4 eV (Fig. 3C), which is assigned to the characteristic peaks of $Cu2p^{3/2}$ and $Cu2p^{1/2}$ of $Cu^0$, respectively [27,28]. From the TEM images (Fig. 3D and E), dark dots with diameter of 3–4 nm were seen on the $TiO_2$ particles, which should belong to the copper clusters. Cu (111) crystal face was clearly discerned from HR–TEM image, and the distance of crystal face was d = 0.206 nm (PDF No. 85-1326) (Fig. 3F). HR–TEM results accompanied by UV–vis DRS, XRD and XPS all indicate the $Cu^0$ is the only product of $Cu^{2+}$ reduced by conduction band electrons ($e_{CB}^-$) of $TiO_2$ under UV light.

To investigate the state of copper species under turnover conditions, *in-situ* UV–vis DRS of $TiO_2$ suspensions with $Cu^{2+}$ was examined after irradiation ($\lambda > 360$ nm) of different time under anaerobic conditions. Consistent with *ex-situ* powder samples (Fig. 3A), a new absorption peak at 578 nm appeared and the intensity rapidly increased with the irradiation, which are assigned to the generation of $Cu^0$ from the reduction of $Cu^{2+}$ by photoinduced eCB-. In addition, a broad absorption at wavelength above 400 nm was observed, which stems from the accumulated $e_{CB-}$ in $TiO_2$. After 65 min irradiation, where all the $Cu^{2+}$ was reduced to $Cu^0$ and the electron accumulation was saturated, the deaerated BDE209 solution was quantitatively dropped into these suspensions under anaerobic conditions. After the reaction in dark, the absorption intensity of accumulated $e_{CB-}$ was markedly decreased, and concomitantly the decrease of BDE209 and the formation of its lower brominated congeners were observed (Fig. S3). However, the peak of $Cu^0$ at 578 nm remained unchanged (Fig. 4), indicating that the copper species remain its zero-valent state under photocatalytic turnover conditions.

### 3.3. Mechanistic discussion on Cu co-catalyzed debromination

In previous reports, both the $Cu^+$ and $Cu^0$ have been reported to catalyze the coupling reaction of halogenated organic compounds through Cu inserting into C–Br bond [29,30]. To distinct which is the real co-catalyst in the photocatalytic debromination, the degradation of BDE209 was investigated by adding $Cu^+$ into the system, and the results are shown in Fig. S4. Without irradiation, no reac-

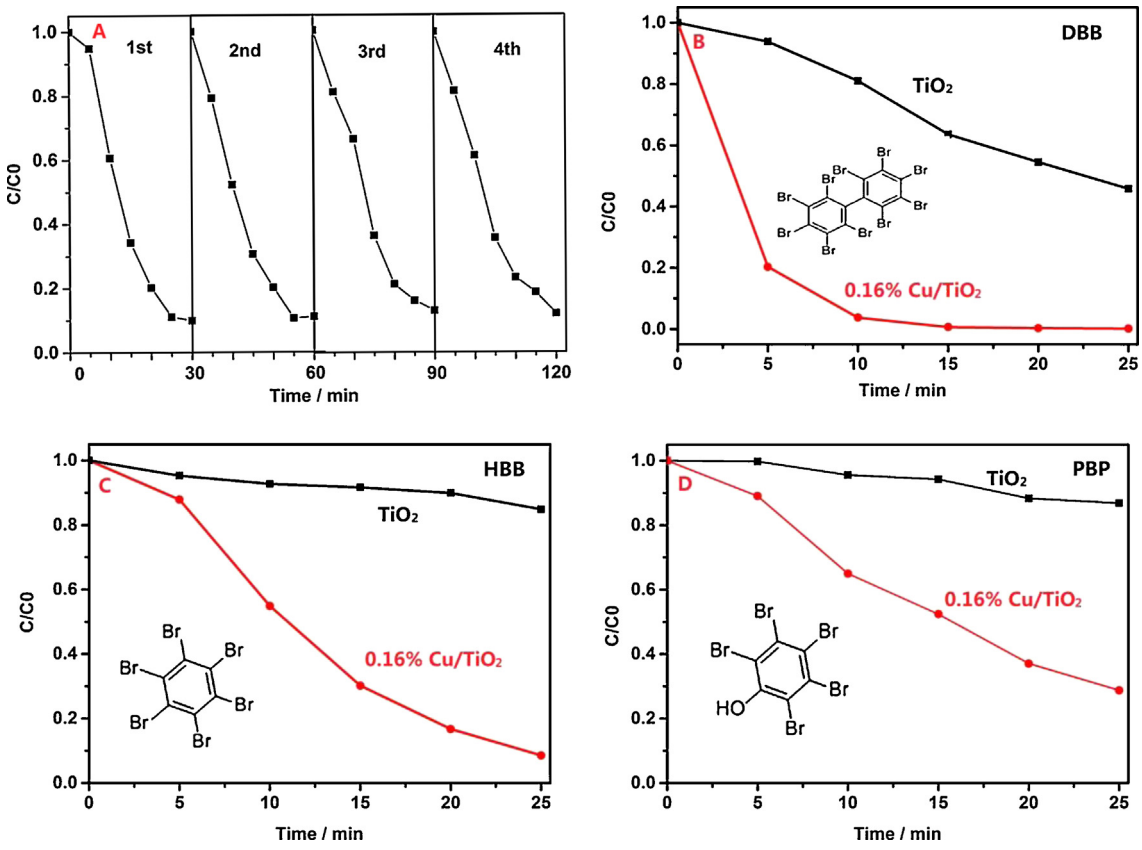


**Fig. 2.** (A) Photocatalytic debromination of BDE209 four times on $Cu^{2+}/TiO_2$, λ > 360 nm; photocatalytic debromination activities on (B) DBB, (C) HBB, (D) PBP on $TiO_2$ and $Cu/TiO_2$, respectively.

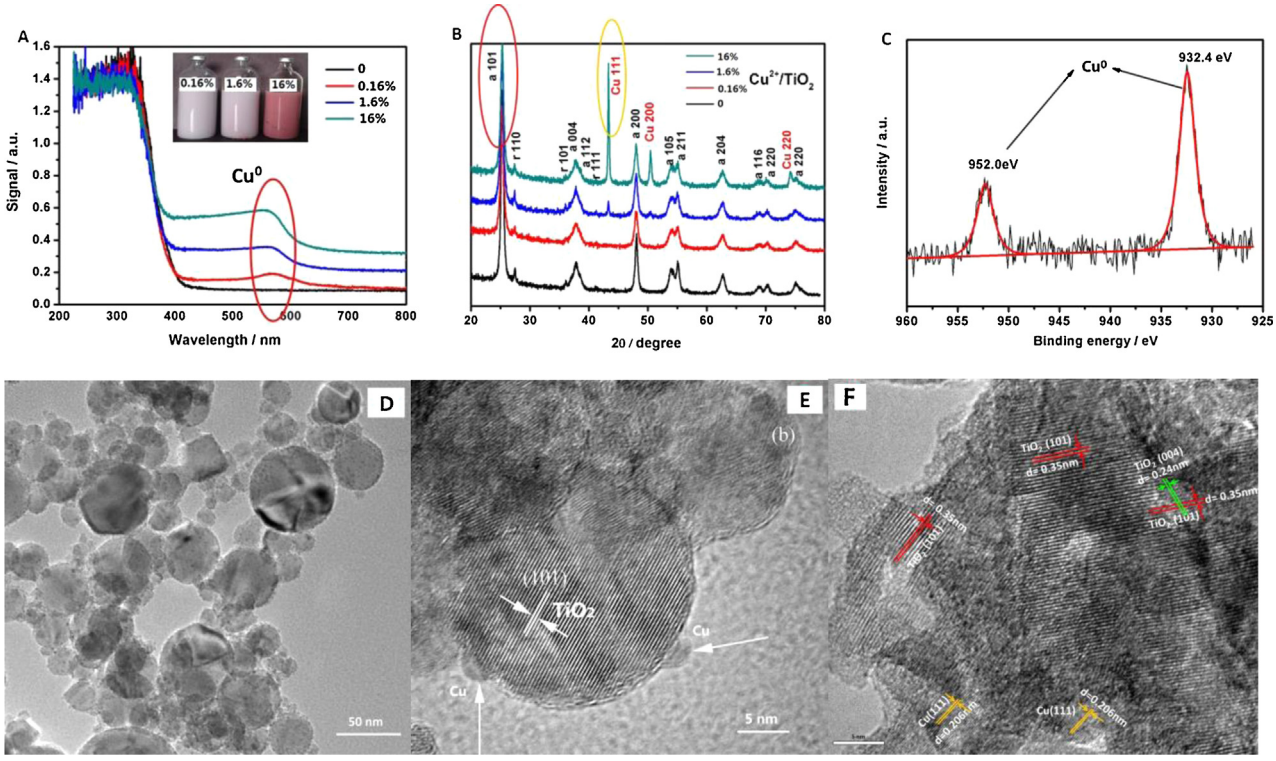


**Fig. 3.** (A) The UV–vis DRS of $TiO_2$ and $Cu/TiO_2$ powders, the inset shows the color change of the $Cu/TiO_2$ suspensions; (B) the XRD spectra of $TiO_2$ and $Cu/TiO_2$ samples; (C) XPS spectra of Cu $2p^3$ of the fresh prepared $Cu/TiO_2$ nanoparticles; (D–F) TEM and HR–TEM image of $Cu/TiO_2$ particles, respectively (for interpretation of the references to color in this figure legend, the reader is referred to the web version of this article).

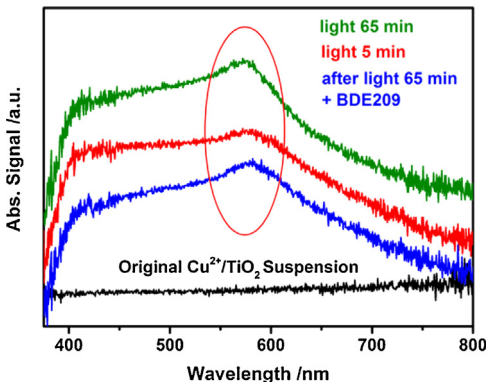


**Fig. 4.** The change of UV–vis DRS spectra after irradiation under anaerobic conditions and the addition of the deaerated BDE 209.

tion for BDE209 in $Cu^+$ alone nor $Cu^+/TiO_2$ systems was observed, indicating that $Cu^+$ is not an active species (neither acts as a catalyst nor as a reagent) for the debromination reaction under the present conditions, although the $Cu^+$ has been reported to hydrodebrominate the dibromoanilines in acidic medium at 90 °C [32]. However, upon light irradiation (λ > 360 nm), $Cu^+/TiO_2$ systems exhibited significant photocatalytic debromination activity, which is attributed to the formation of $Cu^0$ on $TiO_2$ due to $Cu^+$ reduction by $e_{CB}^-$. On the other hand, the coexistence of the BDE209 and metal Cu after the depletion of $e_{CB}^-$, as shown in Figs. 4 and S3, imply that metal Cu particles themselves are inactive for the reduction of BDE209, in the absence of $e_{CB}^-$. Two pathways can be invoked to interpret the cocatalytic effect of metal Cu particles: (1) metal Cu particles mediate directly the electron transfer from the conduction band to BDE209, without explicit change in the chemical state of Cu; (2) the $e_{CB}^-$ reduce $Cu^{2+}$ to $Cu^+$ or $Cu^0$ which will cleave the C—Br bond first and return themselves to $Cu^{2+}$. The inertness of $Cu^+$ and $Cu^0$ towards debromination excludes the second possibility. Accordingly, the enhancive effects of Cu should be attributed to $Cu^0$-mediated electron transfer. Furthermore, the influence of the surface area change after $Cu^0$ loaded on $TiO_2$ can be ruled out. Due to after $Cu^0$ has been loaded on $TiO_2$ surface, the surface area shows slightly decrease from 116 $m^2/g$ of bare $TiO_2$ to 103 $m^2/g$ of $Cu/TiO_2$, which is unfavorable for the enhancement of the photocatalytic activity.

After showing that Cu species is in the form of metal Cu under turnover conditions, we tried to uncover the specific role of $Cu^0$ on the photocatalytic debromination. First, the effect of $Cu^0$ particles on the adsorption of BDE209 was examined by monitoring the concentration of BDE209 in the presence of pre-loaded $Cu/TiO_2$ under different conditions. As indicated in Fig. 5A, the addition of BDE209 in the pre-loaded $Cu/TiO_2$ suspension would lead to an immediate decrease of BDE209 (about 50%) and the formation of low brominated congers (Fig. S5), which is due to the reduction of BDE209 by pre-stored $e_{CB}^-$ as shown in Figs. 4 and S3. After further stirring 30 min in Ar and in dark, the concentration of BDE209 was further decreased by 25% relative to the residual BDE209, with small decrease in the amount of 9-Br congeners. The decrease of BDE209 should result dominantly from its adsorption, but not from its further reduction since no 9-Br congeners was formed. Interestingly, when the suspension was exposed to the air, the concentration of BDE209 in the solution increased by about 7%, with small increase in the amount of 9-Br congers, which is a clear evidence for its desorption from the photocatalyst surface. In the air, the surface of the metal Cu particles is gradually covered by copper oxides $CuO_x$ due to the oxidation of $Cu^0$ by the $O_2$. Accordingly, the increase in the concentration of BDE209 indicates that the metal Cu particles have much higher adsorption ability for the hydrophobic BDE209 than the copper oxides. In contrast, the adsorption of BDE209 on $TiO_2$ was undetectable because of its weak interaction with the strongly hydrophilic surface of $TiO_2$.

From the UV–vis DRS spectra (Figs. 3 A and 4), there was a broad visible light absorption band centered at 578 nm, due to the SPR of metal Cu nanoparticles. It is known that the SPR properties of the noble metal particles such as Au can be used to initiate many photochemical reactions by using visible light [33]. We wonder whether the SPR of metal Cu particles can contribute to the enhanced debromination on $Cu/TiO_2$. To examine visible light activity of Cu particles, the photocatalytic reduction of BDE209 in $Cu/TiO_2$ suspension was carried out under different irradiations. Since the SPR absorption of Cu nanoparticle ranged from 400 nm to 700 nm with maximum at 578 nm, we firstly used a visible light source with λ > 450 nm to selectively excite the SPR of Cu but avoid the direct excitation of $TiO_2$ photocatalyst. In this situation, little degradation of BDE209 was observed (Fig. 5B), indicating the inactivity of the SPR of Cu metal particles alone for the debromination. Interestingly, when a UV (λ = 365 nm) light was employed to excite the $TiO_2$ and a visible light was used at the same time, the reaction rate under the two-light-source irradiation was much higher than that under UV irradiation alone, which implies that the SPR-based visible light absorption of Cu particles can promote the UV-induced debromination, although SPR of metal Cu itself is inactive. In the $Cu/TiO_2$ photocatalyst, the photogenerated eCB- of $TiO_2$ (about −0.29 V *vs.* NHE) can be trapped by the metal Cu particles (with original Fermi level of about 0.15 V *vs.* NHE). [34] Although the electrons in Cu particles can transfer to BDE209 substrates in dark as discussed above, the visible-light-induced SPR excitation of Cu particles with these electrons would largely accelerate the dissociative electron transfer, because the obtained hot-electrons should be more active for the debromination. It is notable that, in the present study, we used a Xe lamp as the light source whose radiation includes both the UV light and visible light. The visible light fraction can contribute to the activity enhancement of $Cu^0/TiO_2$ by the SPR absorption of Cu particles, and the schematic diagram of photoreductive debromination on $Cu/TiO_2$ is shown in Fig. 7.

During the photocatalytic debromination process, the intermediate products of BDE209 reduction over bare $TiO_2$ and *in-situ* $Cu/TiO_2$ systems were investigated by the GC–μECD. It was observed that the decay of BDE209 is a step wise debromination process to its low brominated congeners. After the loss of the first bromine atom, three nona-BDE congeners were generated, which are corresponding to the removal of bromine atom from the *ortho*–(BDE206), *meta*–(BDE207) and *para*–position (BDE208) of BDE209, respectively, in both systems (Fig. 6A). However, at the similar reduction rate of BDE209 (Fig. S6), the relative distributions of three nona–BDEs products were quite different between them. On bare $TiO_2$, the formation of BDE206 was apparently preferential to that of BDE207 and BDE208, indicating that the bromine atom at *ortho*–position is easier to release over bare $TiO_2$. In contrast, for $Cu/TiO_2$ system, BDE207 and BDE208 were the main products, and only very small amount of BDE206 was produced, implying that the *meta*– and *para*–position bromine atoms are susceptive in $Cu/TiO_2$ system.

The three nona-BDE congeners will be further photoreduced debromination, leading to the formation of various octa-BDEs products. Fig. 6B shows the dominant octa–BDE congeners. Over $TiO_2$, consistent with the earlier study [22], the main detected octa–BDE intermediates were BDE198 (2,3,3′,4,5,5′,6,6′–BDE), BDE199 (2,3,3′,4′,5,5′,6,6′–BDE) and BDE196 (2,3′,4,4′,5,5′,6,6′–BDE). In all these three major octa–BDE congeners, at least one of the lost bromine atoms is from the *ortho*–position. However, in $Cu/TiO_2$ system, the main octa–BDE congeners were BDE204 (2,2′,3,4,4′,5,6,6′–BDE), BDE197(2,2′,4,4′,5,5′,6,6′–BDE) and BDE201 (2,2′,3,4′,5,5′,6,6′–BDE) [25], which are all correspond-

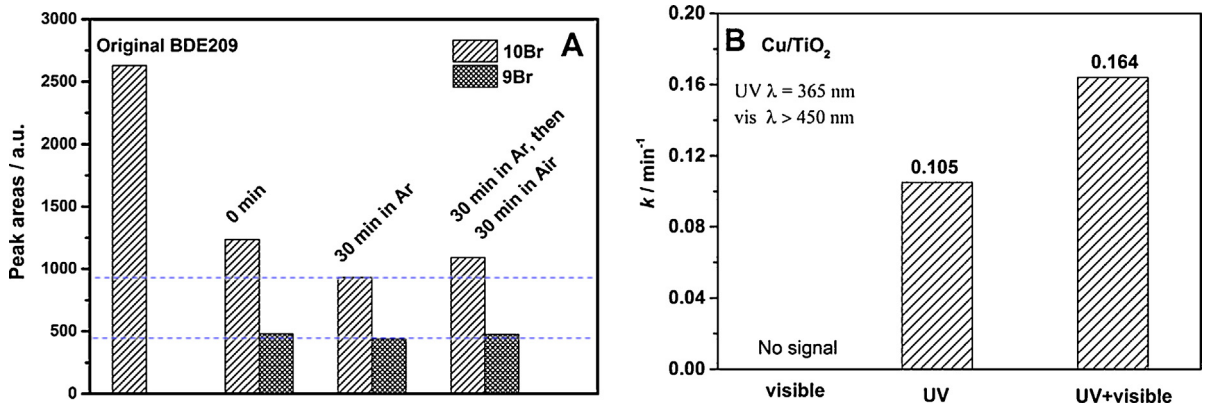


**Fig. 5.** (A) Enhanced adsorption of BDE209 by $Cu^0$ particles. (The change of BDE209 concentration: after added in $Cu^0/TiO_2$ system with saturated electron and stirring 30 min in Ar, then further stirring 30 min in air without irradiation.) (B) The reaction rate constant *k* of BDE209 over $Cu/TiO_2$, under visible, UV and UV + visible light irradiation, respectively. UV: λ = 365 nm, vis: λ > 450 nm.

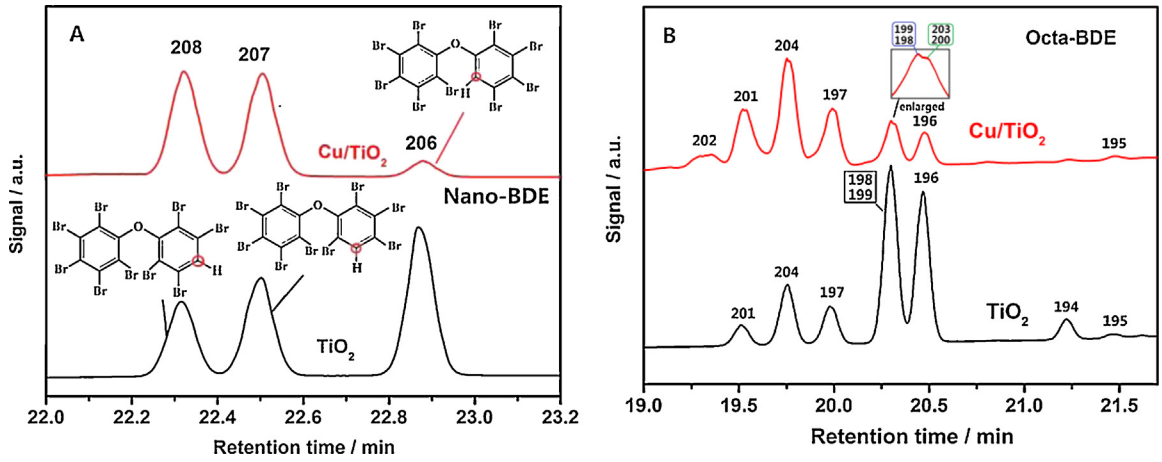


**Fig. 6.** Difference of intermediates (A) nona−BDE and (B) octa−BDE congeners during the photoreductive debromination of BDE209 on $TiO_2$ and $Cu/TiO_2$.

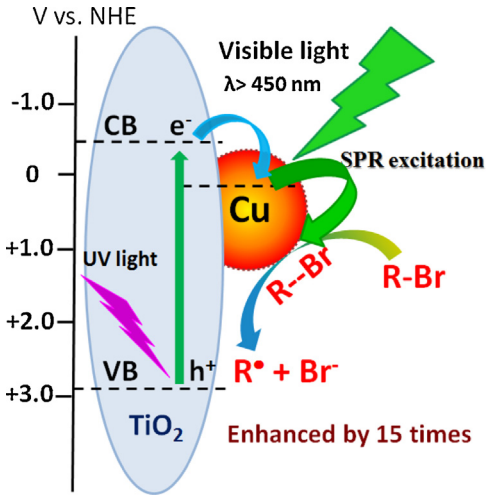


**Fig. 7.** The schematic diagram of photoreductive debromination of bromo-aromatic compounds on $Cu/TiO_2$.

ing to the debromination of *para*− or *meta*−positions, whereas all the *ortho*−position bromine atoms remained untouched.

The debromination reaction of BDE209 involves two-electron transfer. It is generally accepted that the debromination rate is determined by the first electron transfer and cleavage of C—Br bond (dissociatve electron transfer). The interaction between the hydrophobic BDE209 and the hydrophilic surface of bare $TiO_2$ is quite weak. Therefore, the electron transfer should occur through an outer sphere mechanisms on bare $TiO_2$. In this process, the electron transfer leads to the formation of a radical anion of BDE209, which is followed by cleavage of C—Br bond. Consequently, the formed nona−BDE intermediates were mainly BDE206 corresponding to the rupture of the weakest *ortho* C—Br bond [22]. However, in $Cu/TiO_2$ system, the debromination is not from the weakest *ortho* C—Br bond, but from the *meta* and *para* C—Br bonds (forming BDE207 and 208) with higher bond dissociation energy (Fig. 6A). The different products distributions indicate a distinct reduction mechanism between $Cu/TiO_2$ and bare $TiO_2$ systems. Possibly, the dissociative electron transfer mechanisms is shifted from the outer sphere route on bare $TiO_2$ to inner sphere one in the presence of metal Cu particles. In fact, the strong interaction between the BDE209 and the $Cu^0/TiO_2$ system particles (Fig. 5A) would change largely the kinetics and/or thermodynamics properties of the dissociative electron transfer, and favor the inner-sphere electron transfer. The inner-sphere electron transfer from the conduction band to the pre-interacted BDE209 would be significantly rapider with respect to the outer sphere route.

A spection on the steric structure of the BDE209 molecule indicates that the *ortho* C—Br bonds of BDE209 have larger steric hindrance. As a result, its interaction with the surface of metal Cu should be weaker than that of the *meta* and *para* ones, which is well consistent with the observations that little nano-BDE congers from *ortho*-debromination was produced. The C—Br is activated to some

extent by its interaction with the surface sites of metal Cu, which would lower the activation free energy for the dissociatve electron transfer. It is also plausible that the electron transfer and cleavage of the C—Br occur in the concerted manner on the surface of metal Cu (Fig. 7), which emphasizes the catalytic effect of metal Cu for the reductive debromination by strong interfacial interaction [32,35].

## 4. Conclusions

The enhanced photocatalytic debromination activities of $Cu/TiO_2$ on polybrominated compounds are attributed to three factors: the strong interaction between the hydrophobic BDE209 and the surface of metal copper, the catalytic effects of metal copper to activate the C—Br during the dissociative electron transfer, and the utility of visible light by the SPR of metal copper particles. Considering that organobromide pollutants are ubiquitous in the environments, there are urgent requirement for elimination techniques. The enhancement of the photocatalytic debromination of PBDEs and other organobromides (DBB, HBB and PBP) by the *in-situ* formed cheap metal copper would be practically favored. The unique property of Cu effects that enhance the hydrophobic PBDEs, catalyze reductive cleavage of C—Br would be applicable to other reductive dehalogenation techniques such as zero−valent iron (ZVI) and electrochemistry.

## Acknowledgements

The authors are grateful for the financial supports of this work from 973 Project (2013CB632405) and NSFC (Nos. 21525729, 21277147, 21407153, 21221002) and the “Strategic Priority Research Program” of CAS (No. XDA09030200).

## Appendix A. Supplementary data

Supplementary data associated with this article can be found, in the online version, at http://dx.doi.org/10.1016/j.apcatb.2016.04.053.

## References

[1] J.P. Dietrich, S.A. Strickland, G.P. Hutchinson, A.L. Van Gaest, A.B. Krupkin, G.M. Ylitalo, M.R. Arkoosh, Environ. Sci. Technol. 49 (2015) 3878–3886.
[2] C.A. de Wit, Chemosphere 46 (2002) 583–624.
[3] R. Airaksinen, A. Hallikainen, P. Rantakokko, P. Ruokojärvi, P.J. Vuorinen, J. Mannio, H. Kiviranta, Environ. Sci. Technol. 49 (2015) 3851–3859.
[4] L.G. Costa, G. Giordano, S. Tagliaferri, A. Caglieri, A. Mutti, Acta. Biomed. 79 (2008) 172–183.
[5] C.G. Coburn, M.C. Curras-Collazo, P.R.S. Kodavanti, Neurochem. Res. 33 (2008) 355–364.
[6] J.D. Meeker, P.I. Johnson, D. Camann, R. Hauser, Sci. Total Environ. 407 (2009) 3425–3429.
[7] K.S. Betts, Environ. Sci. Technol. News 36 (2002) 50–52.
[8] B. Eskenazi, J. Chevrier, S.A. Rauch, K. Kogut, K.G. Harley, C. Johnson, C. Trujilo, A. Sjödin, A. Bradman, Environ. Health Perspect. 121 (2013) 257–262.
[9] D.E. Buttke, A. Wolkin, H.M. Stapleton, M.L. Miranda, J. Expo. Sci. Environ. Epidemiol. 23 (2013) 176–182.
[10] H.M. Stapleton, S. Eagle, R. Anthopolos, A. Wolkin, M.L. Miranda, Environ. Health Perspect. 119 (2011) 1454–1459.
[11] P.D. Noyes, H.M. Stapleton, Endocr. Disrupt. 2 (1–25) (2014) e29430.
[12] J.B. Manchester-Neesvig, K. Valters, W.C. Sonzogni, Environ. Sci. Technol. 35 (2001) 1072–1077.
[13] M.J. Laguardia, R.C. Hale, A. Harvey, Environ. Sci. Technol. 41 (2007) 6663–6670.
[14] H.M. Stapleton, B. Brazil, D. Holbrook, C.L. Mitchelmore, R. Benedict, A. Konstantinov, D. Potter, Environ. Sci. Technol. 40 (2006) 4653–4658.
[15] J.A. TokarzIII, M.Y. Ahn, J. Leng, T.R. Filley, L. Nies, Environ. Sci. Technol. 42 (2008) 1157–1164.
[16] Y.S. Keum, Q.X. Li, Environ. Sci. Technol. 39 (2005) 2280–2286.
[17] K. Yu, C. Gu, S.A. Boyd, C. Liu, C. Sun, B.J. Teppen, H. Li, Sci. Technol. 46 (2012) 8969–8975.
[18] Z. Xiong, D. Zhao, G. Pan, Water Res. 41 (2007) 3497–3505.
[19] L. Granelli, J. Eriksson, M. Athanasiadou, A. Bergman, Chemosphere 82 (2011) 839–846.
[20] C. Cui, X. Quan, S. Chen, H. Zhao, Sep. Purif. Technol. 47 (2005) 73–79.
[21] K. Nose, S. Hashimoto, S. Takahashi, Y. Noma, S. Sakai, Chemosphere 68 (2007) 120–125.
[22] C.Y. Sun, D. Zhao, C.C. Chen, W.H. Ma, J.C. Zhao, Environ. Sci. Technol. 43 (2009) 157–162.
[23] C.Y. Sun, J.C. Zhao, H.W. Ji, W.H. Ma, C.C. Chen, Chemosphere 89 (2012) 420–425.
[24] L.N. Li, W. Chang, Y. Wang, H.W. Ji, C.C. Chen, W.H. Ma, J.C. Zhao, Chem. Eur. J. 20 (2014) 11163–11170.
[25] H. Wei, R.Q. Yang, A. Li, E.R. Christensen, K.J. Rockne, J. Chromatogr. A 1217 (2010) 2964–2972.
[26] A.N. Pestryakov, V.P. Petranovskii, A. Kryazhov, O. Ozhereliev, N. Pf änder, A. Knop-Gericke, Chem. Phys. Lett. 385 (2004) 173–176.
[27] H.O.A. Fredriksson, E.M. Larsson Langhammer, J.W. Niemantsverdriet, J. Phys. Chem. C 119 (2015) 4085–4094.
[28] J.L. Gong, H.R. Yue, Y.J. Zhao, S. Zhao, L. Zhao, J. Lv, S.P. Wang, X.B. Ma, J. Am. Chem. Soc. 134 (2012) 13922–13925.
[29] E. Sperotto, G.P.M. van Klink, G. van Koten, J.G. de Vries, Dalton Trans. 39 (2010) 10338–10351.
[30] A.A. Isse, A. Gennaro, C.Y. Lin, J.L. Hodgson, M. Coote, T. Guliashvili, J. Am. Chem. Soc. 133 (2011) 6254–6264.
[31] M. Lei, N. Wang, L.H. Zhu, Q.L. Zhou, G. Nie, H.Q. Tang, Appl. Catal. B: Environ. 182 (2016) 414–423.
[32] B. Liedholm, Acta Chem. Scand. B 38 (1984) 877–884.
[33] H.Y. Zhu, X.B. Ke, X.Z. Yang, S. Sarina, H.W. Liu, Angew. Chem 122 (2010) 9851–9855.
[34] D.R. Lide, CRC Handbook of Chemistry and Physics, 88, 2008.
[35] A.A. Isse, S. Gottardello, C. Durante, A. Gennaro, Phys. Chem. Chem. Phys. 10 (2008) 2409–2416.